

Electronic Supplementary Information for

Revealing the Role of Surface Elementary Doping in Photocatalysis

Danlu Yang,^{a,b} Zhijian Wang,^{*a,b} and Jiazang Chen^{*a,b}

^aState Key Laboratory of Coal Conversion, Institute of Coal Chemistry, Chinese Academy of Sciences,
Taiyuan 030001, China

^bCenter of Materials Science and Optoelectronics Engineering, University of Chinese Academy of
Sciences, Beijing 100049, China

* Author to whom correspondence should be addressed.

Email: chenjiazang@sxicc.ac.cn (J.C.); wangzhijian@sxicc.ac.cn (Z.W.)

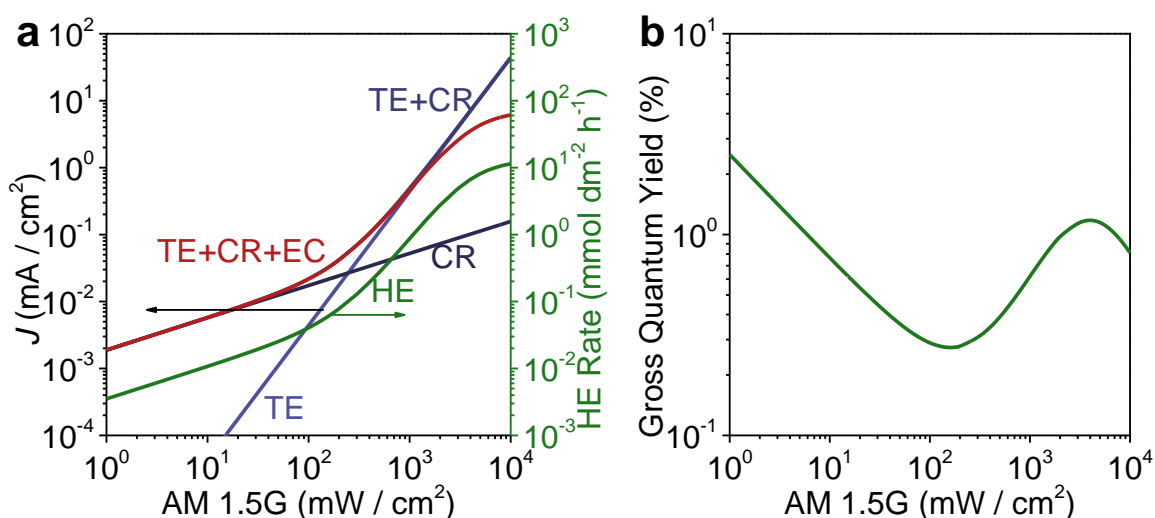


Figure S1. Simulation of light-intensity-dependent SC and semiconductor-cocatalyst-solution (SCS) interfacial electron transfers. Under intense irradiation, SC interfacial electron transfer is predominated by thermionic emission (TE), and the current increase quadratically with the incident photons (a).¹ Under weak illumination, the current is proportional to the square root of the incident photons, because charge recombination (CR) is the major behavior for SC interfacial electron transfer (a).¹ By considering the electrochemical step (EC) occurred on the cocatalyst, the current for SCS interfacial electron transfer (TE+CR+EC) that reflects photocatalytic reduction half-reaction (e.g.: hydrogen evolution, HE) decreases in the extremely intense light region (a). This is because the electrochemical step requires considerable potential drop in this region.^{2,3} By combining the power-law dependence of thermionic emission and charge recombination on light intensity, the transition of interfacial electron transfer behaviors makes the photon utilization encounter a minimum near the standard sunlight (b). Parameters adopted for the simulation: barrier height for metal-semiconductor contact, $\varphi_B = 1.65$ eV; relative permittivity, $\varepsilon_r = 5.7$; effective absorption of photons, $A = 100$ % of photons integrated from ultraviolet region to 517 nm (for the absorption boundary of CdS) in the solar spectrum (AM 1.5G); effective mass of electrons, $m_e^* = 2.46 \times 10^{-31}$ kg; exchange current of hydrogen evolution, $J_0 = 3$ mA/cm²; temperature, $T = 298$ K.

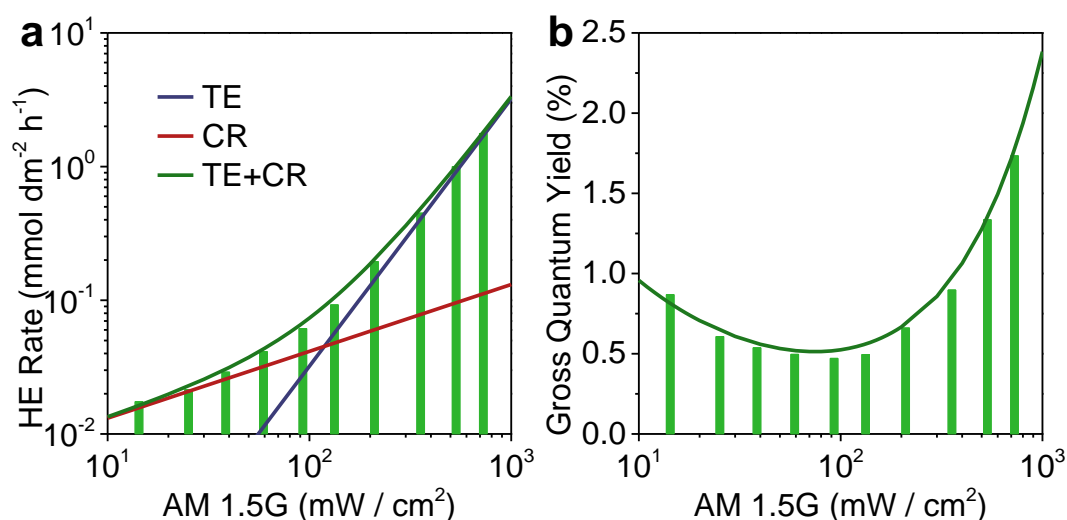


Figure S2. Photocatalytic behaviors of the Pt/CdS photocatalyst in aqueous solution of lactic acid.

Under intense irradiation (e.g.: $>200 \text{ mW cm}^{-2}$), HE rates (experimental data, column bars) vary quadratically with the light intensity (a), suggesting thermionic emission (TE) predominates CdS-Pt interfacial electron transfer. Under weak illumination, the slope of HE rates (experimental data, column bars) over the light intensity is only slightly higher than 0.5, because charge recombination (CR) mainly accounts for the interfacial electron transfer (a). By superposing the simulated data, the curve TE+CR fits well with the experiment data (a). The gross quantum yields that reflect the photocatalytic utilization of incident light exhibit a minimal value at $\sim 100 \text{ mW cm}^{-2}$ along the variation of irradiation intensity (b). The gross quantum yields are the numeric ratios of electrons for HE to the effective incident photons. The effective photon flux was estimated by integrating the incident photons from ultraviolet region to the threshold absorption boundary (517 nm for CdS) in the solar spectrum (AM 1.5 G). The gross quantum yields obtained from the incident light with continuous wavelength can match well the value that from monochromic photons.⁴ The hydrogen evolution behaviors (column bars) were replotted from the experimental data shown in Figure 5 (Mn-0).

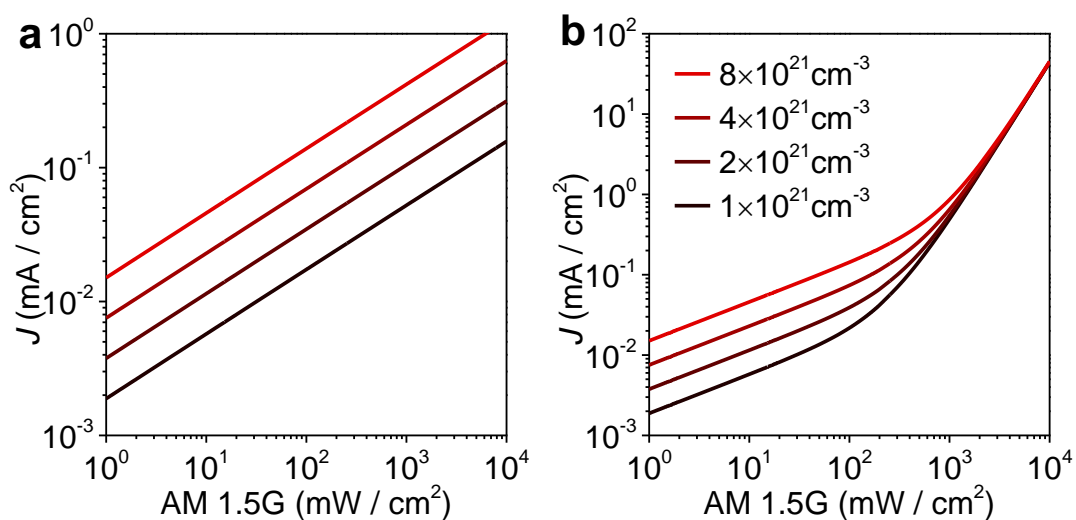


Figure S3. Simulation of light-intensity-dependent semiconductor-cocatalyst interfacial electron transfer by charge recombination with influence of density of surface states (a) and the combined current contains the contribution by thermionic emission (b). The parameters adopted for the simulation: density of electronic doping, $N_d = 1, 2, 4,$ and $8 \times 10^{21} \text{ cm}^{-3}$; other parameters can be found in Figure S1.

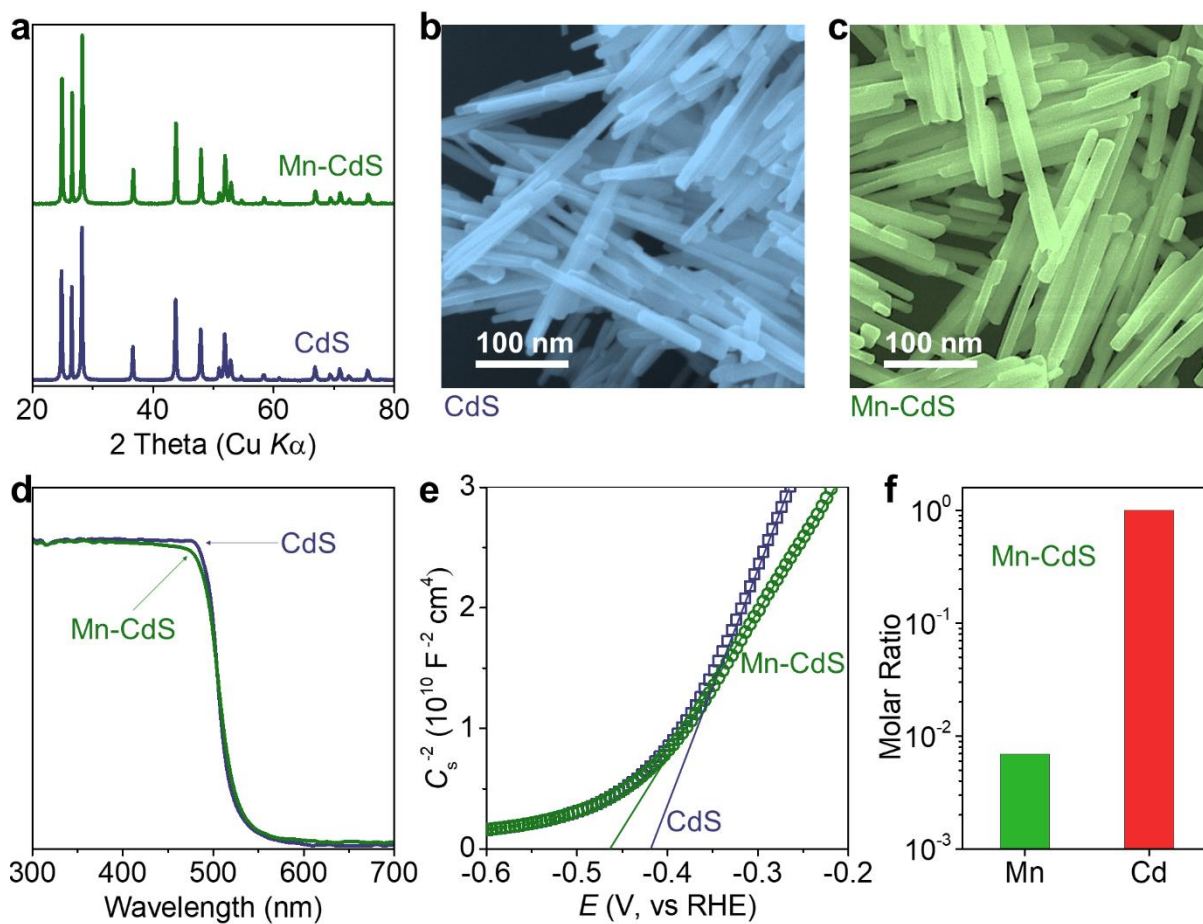


Figure S4. X-ray diffraction patterns (a), electron microscopy images (b, c), light absorption spectra (d), and Mott-Schottky curves (e) for the CdS with and without manganese doping. The elementary analysis obtained from ICP-OES shows that the molar ratio of Mn: Cd is 0.0096: 1 in the formed Mn-CdS (f).

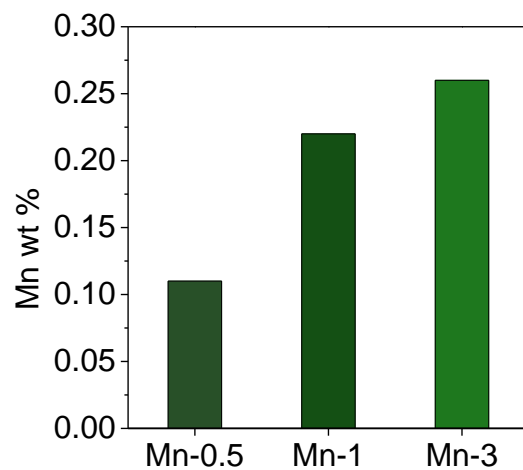


Figure S5. Manganese concentration in the CdS nanorods after hydrothermal treatment in manganese-containing solution. The ratio of surface dopant to the total mass of the doped CdS offsets the linearity to the feed molar ratio between manganese in the solution and cadmium in solid (CdS). The feed molar ratios of Mn: Cd are 0.5, 1, and 3 :100 for Mn-0.5, Mn-1, and Mn-3, respectively.

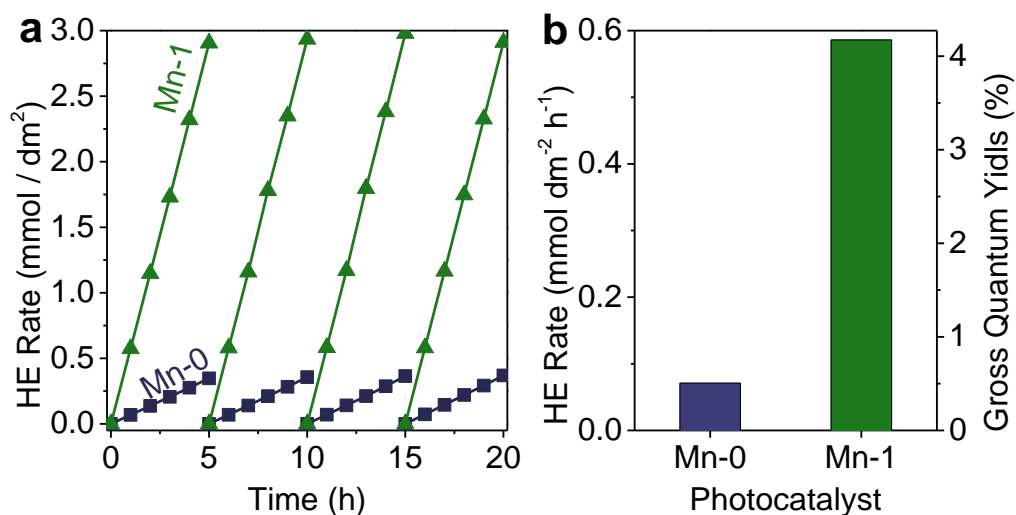


Figure S6. Long-term HE behaviors of platinum loaded CdS with (Mn-1, green triangle) and without (Mn-0, blue square) surface doping under sunlight (A_m 1.5G, 100 mW/cm^2). Both of the photocatalysts exhibit stable hydrogen evolution during the long-term operation (a). As evaluated from the long-term operation, the average HE rate and the gross quantum yields for Mn-1 photocatalyst are 0.586 $\text{mmol dm}^{-2} \text{h}^{-1}$ and 4.17 %, which are 8.25 times higher than that of 0.071 $\text{mmol dm}^{-2} \text{h}^{-1}$ and 0.506 % for Mn-0, respectively (b).

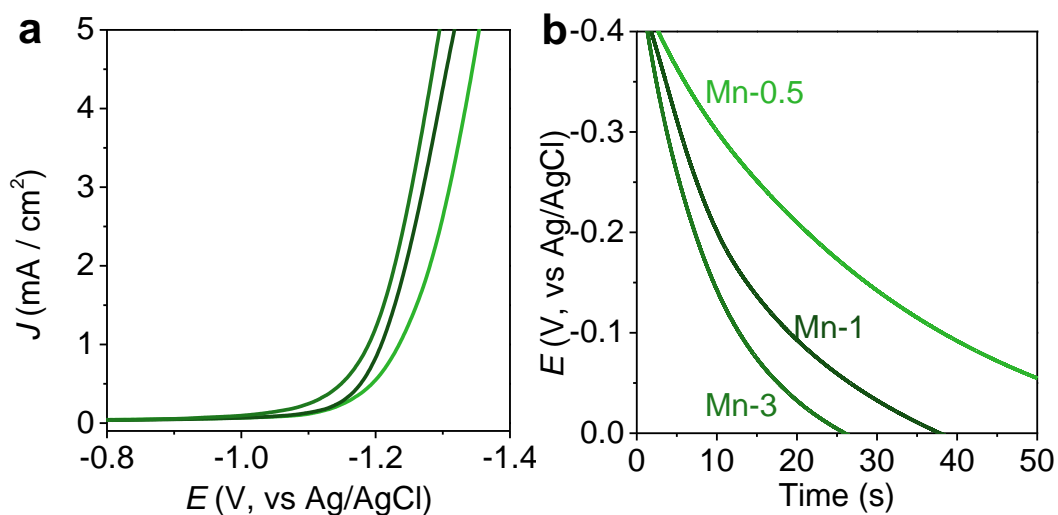


Figure S7. Voltammetry behaviors (a) and decay behaviors of photoinduced open-circuit potential (b) for manganese doped CdS.

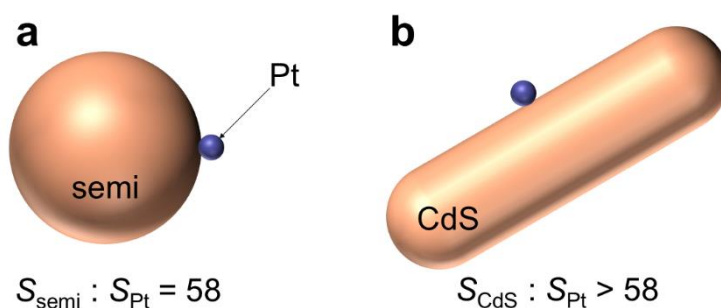


Figure S8. Schematic diagram for semiconducting photocatalyst deposited with cocatalyst. For the photocatalyst CdS nanostructures loaded with 1 wt % of platinum, the volume ratio of CdS to Pt is 445, and the surface area ratio of CdS to Pt reaches as high as 58 (for the semiconductor with spherical structure, a) or even larger (rodlike structure, e.g.: CdS, b). Thus, the percentage for the surface of CdS nanostructures covered by the deposited platinum cocatalyst is very low. When the dopant concentration is high (e.g.: Mn-3), it can hardly cover all the doped area (sites) by platinum. The doped area without platinum deposition will undesirably be the centers of charge leakage.

Simulation

Semiconductor based photocatalytic systems can be treated as integrated photoelectrochemical cells without external potential bias.⁵ Photocatalytic reduction half-reaction like hydrogen evolution mainly composed of two electronic processes, the interfacial transfer of electrons from semiconductor nanostructures to reduction cocatalysts (metal) and electrocatalytic transfer of these electrons to the solution. These two electronic processes are connected in series. Because the electrocatalytic process occurred on cocatalyst like platinum is efficient, photocatalytic reduction half-reaction is dominated by the semiconductor-metal (SM) interfacial electron transfer.⁶ Generally, SM interfacial electron transfer can be the combination of thermionic emission and trap states intermediated charge recombination.⁷ The description for simulation of these electronic processes can be found in our recent publication.^{2,3}

Experimental Procedures

Surface Doping of CdS Nanorods. CdS nanorods were prepared by hydrothermal treatment of cadmium-containing solution in the presence of sulfur resource. In a typical procedure, 20 mmol CdCl₂•2.5H₂O and 60 mmol thiourea were dispersed into 60 mL ethylenediamine. The mixture was then transferred into a Teflon-lined stainless-steel autoclave that was heated at 160 °C for 48 h and allowed to cool down to room temperature. After that, the yellow products were centrifuged and washed with distilled water and ethanol several times, and then dried at 60 °C overnight in vacuum.

Formation of surface doping can be realized by hydrothermal treatment (200 °C, 24 h) of the CdS nanostructures (200 mg) in a Teflon-lined stainless-steel autoclave (100 mL) which had been filled with aqueous solution of MnCl₂ (Mn-0, 0 mM, 60 mL; Mn-0.5, 0.118 mM, 60 mL; Mn-1, 0.236 mM, 60 mL; Mn-3, 0.707 mM, 60 mL). After reaction, the Mn-doped CdS was filtered and washed several times with ethanol and distilled water, followed by vacuum-dried at 60 °C overnight.

Semiconductor (Photo)-Electrochemistry. The Semiconductor (Photo)-Electrochemistry tests were measured in tri-electrode systems, in which a piece of carbon cloth was used as counter electrodes, a liquid bridge containing an inert electrolyte (KCl) was used to connect the reference electrode (Ag/AgCl/Sat. KCl) and the cell.

The procedure for fabrication of semiconductor electrodes for voltammetry measurements can refer to our previous publication with minor modification.^{4,6}

To avoid the direct contact of platinum to the glass carbon, the fabrication of Pt-modified CdS (Mn-CdS) electrodes can be realized by depositing of Pt/CdS (or Pt/Mn-CdS) onto CdS film that was firstly formed on the conducting substrate. To form the blocking CdS film, 4 μ L of the paste (formed by dispersing 3 mg CdS and 100 μ L Nafion solution into 1 mL ethanol) were deposited onto the glassy carbon rotating disc electrode and dried at room temperature. After that, Pt/CdS (or Pt/Mn-CdS) were deposited onto the CdS film to form platinum modified CdS (or Mn-CdS) electrodes. The deposition of Pt/CdS (or Pt/Mn-CdS) onto the CdS films can be realized by dispersing 5 mg photocatalysts (Pt/CdS or Pt/Mn-CdS) and 100 μ L Nafion solution (5 %) into 1 mL ethanol under sonication. Then, 5 μ L of the resulting dispersion were dropped onto the CdS film coated glassy carbon rotating disc electrode and dried at room temperature. Finally, the formed films were baked with infrared light for five minutes and cooled to room temperature.

The electrochemical behaviors are characterized using linear sweep voltammetry with a scanning rate of 5 mV/s when the working electrode is rotated at 1600 rpm in which aqueous solution of lactic acid (15 vol %, Figure 3a) or a buffered solution of disodium hydrogen phosphate and sodium dihydrogen phosphate (pH=7, 0.2 M Na₂HPO₄ 61 vol % + 0.3 M NaH₂PO₄ 39 vol %, Figure 3b, Figure S7a) were used as the electrolyte. All the linear sweep voltammetry measurements were carried

out using glassy carbon rotating disc electrode.

To determine the time constants of electrons in semiconductor with and without loading of metal platinum, we monitor the open-circuit potential decay (OCP) behaviors in the tri-electrode systems, in which aqueous solution of lactic acid (15 vol %, Figure 4b, Figure S7b) were used as the electrolyte. Fabrication of electrodes for OCP measurements can be realized by deposition of 16 μL of the paste (5 mg CdS (Mn-CdS, Pt/CdS or Pt/Mn-CdS) + 100 μL Nafion solution + 1 mL ethanol) onto fluorine-doped tin dioxide (FTO) conducting glass with an active area of 0.38 cm^2 . The illumination for the measurements was provided by a Xe-lamp equipped with AM 1.5G filter.

Mott-Schottky curves (Figure S4e) were obtained by performing potentiodynamical impedance (ac amplitude: 10 mV; constant frequency: 1000 Hz) of the electrodes in 0.5 M Na_2SO_4 solution, in which a piece of carbon cloth was used as counter electrodes, a liquid bridge containing an inert electrolyte (KCl) was used to connect the reference electrode (Ag/AgCl/Sat. KCl) and the cell. Fabrication of electrode can be realized by deposition of 16 μL of the paste [formed by 5 mg CdS (or Mn-CdS) and 100 μL Nafion solution (5 %) that are dispersed into 1 mL ethanol] onto fluorine-doped tin dioxide (FTO) conducting glass with an active area of 0.38 cm^2 . Tangent lines of the Mott-Schottky plots are drawn to obtain the flat band potential.

Materials Characterizations. Morphology of the samples was characterized by scanning electron microscopy (SEM) on a JEOL JSM-7900F field emission electron microscope. Transmission electron microscopy (TEM) investigations were taken with a JEOL JEM-2100 field emission electron microscope operated at 200 kV. Elementary composition distribution map of the samples was characterized by double spherical aberration corrected transmission electron microscope on a FEI Titan Themis G2 operated at 60 kV. X-ray diffraction (XRD) characterization was conducted on a

Bruker D8 X-ray powder diffractometer. The chemical state of the sample elements is analyzed by X-ray photoelectron spectroscopy (XPS) on a Thermo ESCALAB 250XI. The work function and valance band structure of the sample are obtained by ultraviolet photoelectron spectroscopy (UPS) on a Thermo ESCALAB 250XI. The light absorption performance of the samples adopt UV-vis absorption spectrum on a SHIMADZU UV-3600 with a scan range of 300-700nm. Manganese concentration in the CdS nanorods after hydrothermal treatment in manganese-containing solution is carried out by Inductively Coupled Plasma Optical Emission Spect (ICP-OES) on a Thermo iCAP6300.

Supplementary Information References

1. Z. Wang, W. Qiao, M. Yuan, N. Li and J. Chen, *J. Phys. Chem. Lett.*, 2020, **11**, 2369-2373.
2. H. Xiang, Z. Wang and J. Chen, *J. Phys. Chem. Lett.*, 2021, **12**, 7665-7670.
3. H. Xiang, Z. Wang and J. Chen, *J. Chem. Phys.*, 2021, **154**, 221102.
4. Z. Wang, W. Qiao, M. Yuan, N. Li and J. Chen, *J. Phys. Chem. Lett.*, 2020, **11**, 4644-4648.
5. R. Memming, *Semiconductor Electrochemistry*, Wiley-VCH, Weinheim, 2nd edn., 2015.
6. Z. Wang, N. Xue and J. Chen, *J. Phys. Chem. C*, 2019, **123**, 24404-24408.
7. E. H. Rhoderick, *Metal-semiconductor contacts*, Clarendon Press, 1978.